Winding Challenges and Solutions in the INFN Falcon Dipole Project

R.U. Valente, E. Beneduce, A. Bersani, E. Bianchi, M. Bracco, S. Burioli, B. Caiffi, M. Cannavò, N. Ciarchi, G. Crespi, A. Dellacasagrande, E. De Matteis, S. Dotti, S. Farinon, A.P. Foussat, A. Gagno, T. Maiello, S. Mariotto, L. Musenich, R. Musenich, D. Novelli, A. Palmisano, A. Pampaloni, M. Prioli, L. Rossi, *Fellow, IEEE*, A. Ruggiero, N. Sala, C. Santini, M. Sorbi, S. Sorti, M. Statera, and E. Todesco

***Abstract*—The Falcon Dipole is a project led by the Italian Institute of Nuclear Physics (INFN), which aims tofabricate a 12 T short model of a Nb_3Sn cos-theta accelerator dipole as part of the High Field Magnet (HFM) R&D program at CERN [1]. The status of the project is at the fabrication step of the first dummy coil in the industry and, in this paper, the results of the first campaign of winding tests conducted in the industry are presented. The winding process for the Falcon Dipole is challenging because the size of the Rutherford Cable used for the coils is comparable to the bore radius. This results in high bending and torsion stresses, making the cable structure unstable. To address these challenges, the previous 3D model has been modified to improve the winding feasibility. The setup has been prepared to monitor technical parameters that will help in modeling the coil geometry and identifying sources of critical issues. In this paper, the outcomes of the winding campaign are reported and the proposed changes to the coil end design to address the issues that arose are discussed.**

***Index Terms*—Accelerator magnets, dipoles, Nb_3Sn, coil winding, superconducting magnets.**

I. Introduction

FOLLOWING the preliminary tests at CERN using a copper dummy cable [10], the winding trial campaign started at the ASG superconductors facility, where the actual coil production is planned. Since both the winding machine and tooling at ASG differ from those used at CERN, additional testing is essential to determine the appropriate parameters for the real winding process. The first trial at ASG involved winding the complete inner layer of the coil for the first time. This test revealed several critical issues, particularly around the midplane turns. The most significant finding was that the current endspacer design does not align with the natural path of the cable at the coil ends. Forcing the cable to follow this predefined trajectory led to instabilities, resulting in cable pop-outs and de-cabling. The Falcon Dipole [2], [3], [4], [5], [6], [7], [8], [9], [10], [11] design features a two-layer dipole configuration with a 21 mm wide cable wound around a 50 mm bore, resulting in a cable-to-bore ratio of 0.84. This unusually high ratio introduces a largely unexplored parameter space for coil end design. To accommodate this tight geometry, the coil ends require longer end-spacers to ensure a smooth transition of the cable from straight section to the coil heads. To establish a suitable starting point for optimizing 3D coil end model, a test was conducted on a single midplane turn. The results were then compared with the corresponding 3D model. The analysis revealed that, to significantly reduce strain on cable, midplane turn length should exceed 250 mm. This marks a substantial increase from the previous design which featured a length of approximately 150 mm. Consequently, the end-spacers have been redesigned based on a new set of initial parameters. A second winding trial of the whole inner layer has been performed to confirm that the new coil end design approach is suitable for winding such as rigid cable on a mandrel 50 mm in diameter. The following chapters present improvements in terms of both computed parameters and experimental measurements.

Received 28 July 2025; revised 5 September 2025; accepted 29 September 2025. Date of publication 13 October 2025; date of current version 28 October 2025. This work was supported by the NextGeneration EU—Italian National Recovery and Resilience Plan, Mission 4—Component 2—Investment 3.1.—Project name: IRIS, under Grant CUP: I43C21000230006. *(Correspinding author: R.U. Valente.)*

R.U. Valente, G. Crespi, E. De Matteis, S. Dotti, A. Palmisano, M. Prioli, A. Ruggiero, C. Santini, and M. Statera are with the I.N.F.N., Laboratorio Acceleratori e Superconduttività Applicata, 20090 Milano, Italy (e-mail: riccardo.valente@mi.infn.it).

E. Beneduce, M. Cannavò, N. Ciarchi, S. Mariotto, L. Rossi, M. Sorbi, and S. Sorti are with the Università degli Studi di Milano, 20122 Milano, Italy, and also with the I.N.F.N., Laboratorio Acceleratori e Superconduttività Applicata, 20090 Milano, Italy.

A. Bersani, E. Bianchi, S. Burioli, B. Caiffi, A. Dellacasagrande, S. Farinon, A. Gagno, T. Maiello, R. Musenich, and A. Pampaloni are with the I.N.F.N. Sezione di Genova, 16146 Genova, Italy.

M. Bracco and L. Musenich are with the Università degli Studi di Genova, 16146 Genova, Italy, and also with the I.N.F.N. Sezione di Genova, 16146 Genova, Italy.

A.P. Foussat, N. Sala, and E. Todesco are with the European Organization for Nuclear Research, 1211 Geneva, Switzerland.

D. Novelli is with the Università degli Studi di Roma "La Sapienza," 00185 Roma, Italy, and also with the I.N.F.N. Sezione di Genova, 16146 Genova, Italy.

Color versions of one or more figures in this article are available at https://doi.org/10.1109/TASC.2025.3620787.

Digital Object Identifier 10.1109/TASC.2025.3620787

II. Study of the Natural Bending of the Cable

One of the main outcomes of the initial winding tests is that the cable is so rigid that it follows its own path around the mandrel instead of adapting to the spacer shape. Therefore, by measuring the inclination of the cable in the yz-plane (beta angle), it is possible to determine the cable natural disposition on the mandrel. Therefore, a test has been prepared to perform a parametric study of the 'free' cable and to identify a new set of initial parameters for the subsequent coil ends optimization run.

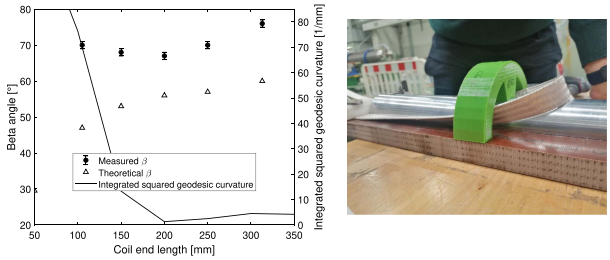

Fig. 1. Results of the parametric test on midplane turn.

The setup consisted of a clamp system to simulate the midplane turn, which experiences the highest torsion and bending and is the longest turn at the coil ends (Fig. 1, right). The main goal of the test was to determine the relationship between the turn length and the beta inclination angle. This angle is measured indirectly by assessing the longitudinal positions of the upper and lower corners of the cable. The experimental results are then compared with a 3D model implemented in ROXIE [13], which has also been used to quantify the level of strain energy in the cable, represented by the integrated squared geodesic curvature [14]. The scatter plot in Fig. 1 shows the comparison between the theoretical and the computed beta angle of the cable: the significant disagreement with the experimental data results from the cable detachment from the mandrel (protrusion), which must be minimized with a proper clamp system during winding. The solid line in the same plot shows that strain energy is heavily reduced for coil ends longer than 200 mm. Considering that the previous version of the coil ends 3D model was $\simeq$150 mm long and the inclination of the midplane block was $\simeq 50°$, it is evident that the model needs to be improved according to the test results.

III. Update of the Coil Ends 3D Model

From the experimental data obtained with the midplane-turn test, guess values are derived for the geometrical parameters to be used as initial inputs for the coil ends optimization in ROXIE software. Based on measurement results, the Falcon Dipole cable, in the worst-case scenario, requires at least 200 mm to be properly accommodated on a 50 mm mandrel. This corresponds to an ellipticity of the base curve of the cable path greater than 5. From the parametric study, it follows that such a large ellipticity requires the hyperellipse order to be greater than 4. This represents an unexplored parameter space in coil ends optimization of cos-theta magnets, compared to the usual values used for other dipoles like the main LHC bending dipoles [15], which employ hyperellipses with ellipticity 1.5 and order 3. Another key feature introduced in the new version is the turn-by-turn variation of the beta inclination angle caused by cable stacking. In ROXIE, it is possible to insert artificial inter-turn wedges between each cable within a block at the coil end. This allows for fine-tuning of the cable positions in the winding by adjusting the major (w_o) and minor (w_i) bases of its trapezoidal cross-section. Typically, these adjustments do not exceed 0.3 mm for the major base. However, the first complete winding test of the inner layer revealed an average turn advancement of approximately 0.75 mm. The parameters used for the last optimization are

TABLE I
Inputs for the Deterministic Multi-Variable and Multi-Objectives Optimization (EXTREM Algorithm)

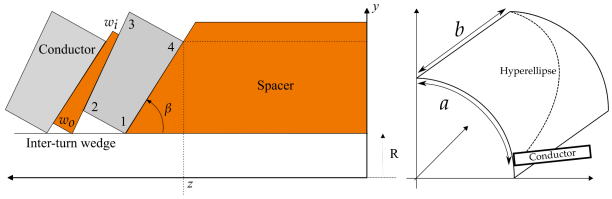

Design variables	Value
Turn inclination to z-axis	$60° < \beta < 75°$
Ellipticity, $f = b/a$	> 5
Hyperellipse order	> 4
Inter-turn wedge dimensions w_o, w_i	0.75 mm, 0.02 mm
Parameters to be minimized	**Weight of minimization**
Torsion, k_t	1000
Hard-way bending, k_g	100
Soft-way bending, k_n	500
Edge of regression	10000

summarized in Table I as design variables, together with the contributions of the cost function to be minimized: torsion, hard and soft way bending, edge of regression violation that avoids intersection between the discretized surfaces used to model the cable. Usually, the larger weight is given to the edge of regression violation to have a realistic cable surface, and to the geodesic curvature to give priority in reducing the hard-way bending. In the case of Falcon Dipole the torsion has a large weight because the experimental observation is that the more the torsion is, the more the pop-outs occur during winding the heads. The same thing has been observed in a parallel winding test performed at CERN on a different design of the Falcon Dipole [16]. The new coil ends model obtained for the inner layer (iteration 3) has been compared with the previous design (iteration 2) and with the coil model of the double collimator dipoles (11 T dipole) of the dispersion suppression region originally planned in the High-Luminosity LHC upgrade. The new configuration significantly improves the geometric design, using the integral of the squared geodesic curvature as a figure of merit, which relates to the strain energy stored in the cable along the head path. The result is also promising when compared to the 11 T dipole, considering it as a theoretical benchmark. The plots in Fig. 2 show the numerical values.

IV. Winding Test Results

The coil layout that is now proposed for the inner layer is tested in a dedicated winding test at ASG superconductors, and the experimental results have been compared with the previous ones. The experimental setup included (i) a stainless steel mandrel 50 mm in diameter, (ii) a set of plastic clamps screwed onto the mandrel to contain the cable radially, (iii) hydraulic presses to push the cable azimuthally both along the straight part and at the coil ends, (iv) a dedicated system for containing the coil end spacers. All components are mounted on a winding table that can rotate around the vertical, longitudinal, and lateral axes. The cable spool is installed on a tensioner that maintains constant tension during all winding and unwinding

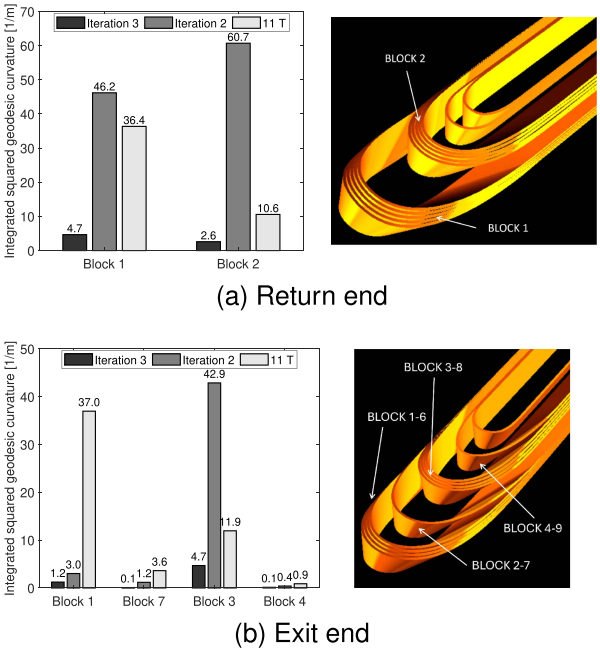

Fig. 2. On the right, the iteration 3 coil end geometry. On the left, the plot of the computed integrated squared geodesic curvature compared with other designs.

phases, moving around the winding table to deposit the cable onto the mandrel. These winding tests were performed using spacers and wedges 3D printed in PLA, enabling fast prototyping between design iterations. The cable used for the tests already has the features of the final design, i.e. bare width and mid-thickness unreacted 20.950±0.002 mm and 1.802±0.001 mm, respectively, with a keystone angle of 0.490±0.005°. The strand twisting is left-handed with a pitch of 110 mm. During the winding trials, the Falcon Dipole dummy cables are used in different configurations: (i) copper not insulated, (ii) copper, and (iii) Nb_3Sn insulated with a braided S2-glass fiberglass 152±5 µm thick under 5 MPa of compression. During the test campaign, it was observed that the bare copper dummy cable is not stable enough to complete the entire inner layer of the coil. The turns toward the midplane are subject to high torsion and bending, which consistently cause strand pop-outs. On the other hand, the braided insulation provides the cable with the necessary stability to prevent strand opening, even in the worst cases. Therefore, only tests with insulated cables are considered significant for validating the design. Additionally, experimental observations indicate that Nb_3Sn cables show higher stability due to the rigidity of their strands, which limits deformation of the cable cross-section and preserves the natural trajectory even with suboptimal spacers. On the other hand, copper cables are softer and can be forced onto non-ideal paths, but this often leads to pop-outs, which provide a clearer diagnostic of whether the spacer geometry conforms to the cable optimal path. Thus, tests performed with copper dummy cables are regarded as more conservative than those conducted with Nb_3Sn cables. Here, the results of two key tests are presented. One was performed on 10th January 2025, on the iteration 2 version of the coil geometry [4], and the other on 27th June 2025, to evaluate

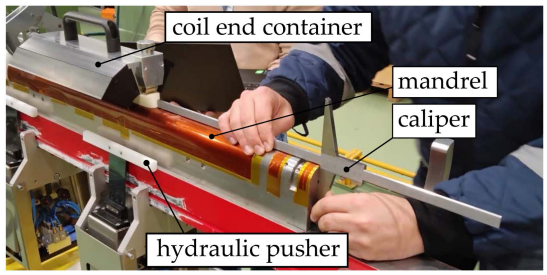

Fig. 3. Measuring operation to determine the beta angle inclination of each turn and spacer.

the iteration 3 version of the spacers, which are designed with the improvements described in section III. In these cases, the iteration 2 spacers were tested with Nb_3Sn-insulated cable, while the iteration 3 version was tested with copper-insulated cable. Both tests were performed with a winding tension of 200 N, winding the cable in its favorable twisting direction, as planned for the inner layer of the coil, to reduce the risk of pop-outs and prevent cable openings. The parameters monitored during the tests were: (a) *Beta inclination angle* in the *yz*-plane, which was indirectly determined by measuring, with a caliper, the distance between a surface plate, positioned at the extremities of the winding machine, and the top and bottom corners of the cable, respectively - the associated measurement error for the angle is estimated at ±1° (Fig. 3); (b) *Protrusion*, defined as the gap between the cable and the mandrel surface, which was measured using a caliper - due to the inherent difficulty of the measurement, an error of ±0.5 mm was considered. At the same time, the quality of the winding was assessed through visual inspection criteria related to cable stability, as described in [17], [18]. In particular, (i) the *pop-outs*, where individual strands are expelled from the cable envelope, (ii) the *tightening*, a misalignment of strands caused by excessive torsion in the cable twist direction, (iii) the *opening*, which is the inverse of tightening, characterized by strand separation, and (iv) the *de-cabling*, a complete loss of the cable structural integrity.

A. Inclination Angle

The most important parameter for monitoring the quality of the coil end is the inclination angle β at the nose of the bend (in the yz-plane). By measuring turn-by-turn, it is possible to compare the experimental data with the expected values from the coil end model and adjust the block geometry if needed. The histograms in Fig. 4 show, in gray bars, the theoretical beta modeled in ROXIE, and in white bars, the experimental data. The turn number axis also includes the spacers, labeled with an acronym that indicates the inner (IL) or outer layer (OL), the return (R) or exit (E) end, and a sequential number starting from 1 (the nose) and increasing until the last one (the end-shoe). The experimental beta angle data of the spacers indicated that the measurement method provides sufficient accuracy to describe the actual trend of cable stacking in the heads. The plot on top of Fig. 4 is the most significant result from iteration 2 of the coil end model, where the theoretical beta angle is assumed to be constant for turns within the same block. However, measurements show

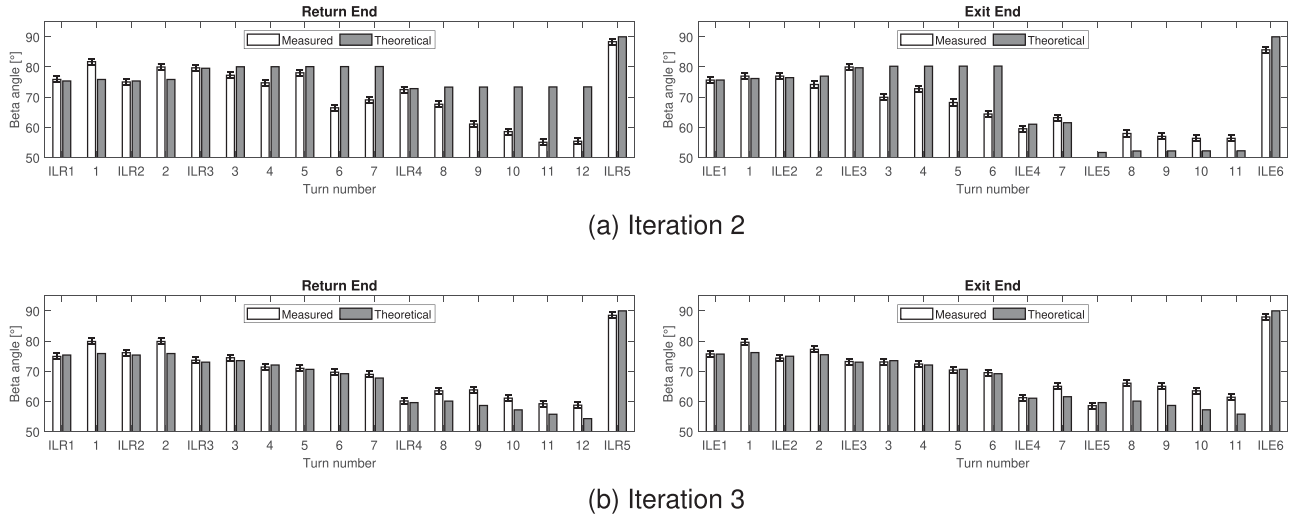

Fig. 4. Inclination beta angle comparison between the iteration 2 and 3 coil model and the experimental measurements.

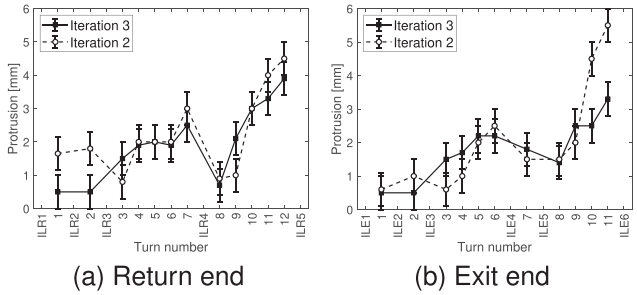

Fig. 5. Experimental data of the protrusion gap.

Iteration 2 - Return Ends

Turn number	Manual torque (Yes/No)	Pop-out (Yes/No)	Opening (Yes/No)	Tightening (Yes/No)	Decabling (Yes/No)
ILR1	N	N	N	N	N
1	N	N	N	N	N
ILR2	N	N	N	N	N
2	N	N	N	Y	N
ILR3	N	N	N	N	N
3	N	Y	N	Y	N
4	N	Y	N	Y	N
5	Y	Y	N	Y	Y
6	N	N	N	Y	N
7	N	N	N	N	N
ILR4	N	N	N	N	N
8	N	Y	N	Y	N
9	N	N	N	Y	N
10	N	N	N	Y	N
11	N	N	N	Y	N
12	N	N	N	Y	N
ILR5	N	N	N	N	N

Iteration 2 - Exit Ends

Turn number	Manual torque (Yes/No)	Pop-out (Yes/No)	Opening (Yes/No)	Tightening (Yes/No)	Decabling (Yes/No)
ILE1	N	N	N	N	N
1	N	N	N	N	N
ILE2	N	N	N	N	N
2	Y	N	N	N	N
ILE3	N	N	N	N	N
3	N	N	N	Y	N
4	N	Y	N	Y	N
5	N	N	N	Y	N
6	N	N	N	Y	N
ILE4	N	N	N	N	N
7	N	N	N	Y	N
ILE5	N	N	N	N	N
8	N	N	N	Y	N
9	N	N	N	Y	N
10	N	N	N	Y	N
11	N	Y	N	Y	N
ILE6	N	N	N	N	N

Iteration 3 - Return Ends

Turn number	Manual torque (Yes/No)	Pop out (Yes/No)	Opening (Yes/No)	Tightening (Yes/No)	Decabling (Yes/No)
ILR1	N	N	N	N	N
1	N	N	N	N	N
ILR2	N	N	N	N	N
2	N	N	N	N	N
ILR3	N	N	N	N	N
3	N	N	N	N	N
4	N	N	N	N	N
5	N	N	N	N	N
6	N	N	N	N	N
7	N	N	N	N	N
ILR4	N	N	N	N	N
8	N	N	N	N	N
9	N	N	N	N	N
10	N	N	N	Y	N
11	N	N	N	N	N
12	N	N	N	N	N
ILR5	N	N	N	N	N

Iteration 3 - Exit Ends

Turn number	Manual torque (Yes/No)	Pop-out (Yes/No)	Opening (Yes/No)	Tightening (Yes/No)	Decabling (Yes/No)
ILE1	N	N	N	N	N
1	N	N	N	N	N
ILE2	N	N	N	N	N
2	N	N	N	N	N
ILE3	N	N	N	N	N
3	N	N	N	N	N
4	N	N	N	N	N
5	N	N	N	N	N
6	N	N	N	N	N
ILE4	N	N	N	N	N
7	N	N	N	Y	N
ILE5	N	N	N	N	N
8	N	N	N	N	N
9	N	N	N	N	N
10	N	N	N	N	N
11	N	N	N	N	N
ILE6	N	N	N	N	N

Fig. 6. Results of the visual inspection during tests.

that the cable naturally tends to decrease its inclination during stacking, with this effect being more evident in the midplane block, specifically from turn 8 to 12 for the return end and from turn 8 to 11 for the exit end. The right turn advancement effect is properly modeled in the iteration 3 version of the coil ends, and the results are reported in the plot at the bottom of Fig. 4. Apart from a systematic under-estimation of the beta angle in the midplane blocks of about 5° that can be easily corrected, the turns fit better the foreseen inclinations.

B. Protrusion

A gap between the cable and the mandrel surface in the coil heads, referred to as *protrusion*, is commonly observed in cos-theta windings, particularly for cables with a large width. Typically, gaps on the order of a few millimeters can be closed by applying pressure during the curing process in the mold. However, the cable rigidity in the hard-way bending direction plays a crucial role in the ease of mold closure operations, and consequently, in the risk of strand damage. In the tests performed on the Falcon Dipole inner layer windings, the protrusion is around 2 mm for the second block (turns 3-7) and 3 mm in the mid-plane block (turns 8-12). The experimental results are shown in the plots in Fig. 5. The iteration 2 and 3 present almost the same level of protrusion, but the last one actually allows to recover the gap using much less force to push down the cable in position, thanks to the fact the turns accumulate less strain energy in their longer trajectory.

C. Visual Inspection

During the tests, each turn was visually inspected to identify any form of cable instability. For the non-insulated cable, this process was straightforward. However, in the case of the insulated cable, the turns had to be physically touched on their accessible surfaces to assess their condition. The Iteration 2 configuration consistently exhibited cable instabilities, especially tightening, but also pop-outs, particularly in the coil block located between the pole and the midplane. These issues were due to improperly fitting spacers, which subjected the cable to significant torsion and bending stresses (Fig. 6). On the other hand, the Iteration 3 design featured longer spacers, allowing the cable to follow a smoother path. This reduced internal mechanical stresses and effectively prevented the occurrence of cable instabilities (Fig. 6).

V. Conclusion

The winding trials and associated analyses presented in this study demonstrate significant progress in the development of the Falcon Dipole inner coil layer. The transition from iteration 2 to iteration 3 of the coil end geometry - driven by a parametric study and validated through experimental testing — has led to improvements in cable stability and enhanced winding quality. The adoption of longer end-spacers and more accurate modeling of the beta inclination angle were critical in fitting the cable natural path with the constraints of the winding geometry. Visual inspections and quantitative data confirm that the updated design minimizes instabilities such as pop-outs and de-cabling, even under conservative testing conditions. These results not only validate the revised 3D model and optimization approach but also provide a solid foundation for the upcoming full-coil production.

References

[1] "High field magnet website," 2025. Accessed: Jul. 18, 2025. [Online]. Available: https://hfm.web.cern.ch/

[2] R. Valente et al., "Electromagnetic and mechanical study for the Nb_3Sn cos-theta Dipole model for the FCC," *IEEE Trans. Appl. Supercond.*, vol. 30, no. 4, Jun. 2020, Art. no. 4001905, doi: 10.1109/TASC.2020.2972219.

[3] A. Pampaloni et al., "Preliminary design of the Nb_3Sn cos-theta short model for the FCC," *IEEE Trans. Appl. Supercond.*, vol. 31, no. 5, Aug. 2021, Art. no. 4900905, doi: 10.1109/TASC.2021.3061334.

[4] R. U. Valente et al., "Update on the electromagnetic design of the Nb_3Sn cos-theta Dipole model for FCC-hh," *IEEE Trans. Appl. Supercond.*, vol. 32, no. 4, Jun. 2022, Art. no. 4001005, doi: 10.1109/TASC.2022.3152100.

[5] R. U. Valente, "Electromagnetic design optimization of the 12 T cos-theta Dipole model for the FCC," PhD Thesis, Sch. Accel. Phys., La Sapienza Univ. Rome, Rome, Italy, 2022. [Online]. Available: https://hdl.handle.net/11573/1668577

[6] R. U. Valente et al., "Study of superconducting magnetization effects and 3D electromagnetic analysis of the Nb_3Sn cosθ short model for FCC," *IEEE Trans. Appl. Supercond.*, vol. 31, no. 5, Aug. 2021, Art. no. 4002205, doi: 10.1109/TASC.2021.3059981.

[7] S. Burioli et al., "COS-THETA Dipole model for the FCC-hh at CERN," 2021. [Online]. Available: http://www.lnf.infn.it/sis/preprint/getfilepdf.php?filename=INFN-22-01-GE.pdf

[8] A. Pampaloni et al., "Mechanical design of FalconD, a Nb_3Sn cos-theta short model Dipole for the FCC," *IEEE Trans. Appl. Supercond.*, vol. 32, no. 6, Sep. 2022, Art. no. 4000605, doi: 10.1109/TASC.2022.3149679.

[9] F. Levi et al., "Updates on the mechanical design of FalconD, a Nb_3Sn cosθ short model Dipole for FCC-hh," *IEEE Trans. Appl. Supercond.*, vol. 33, no. 5, Aug. 2023, Art. no. 4000805, doi: 10.1109/TASC.2023. 3241832.

[10] R. U. Valente et al., "Optimization of electromagnetic design after winding tests for the Nb_3Sn cos-theta Dipole model for FCC-hh," *IEEE Trans. Appl. Supercond.*, vol. 33, no. 5, Aug. 2023, Art. no. 4601107, doi: 10.1109/TASC.2023.3246421.

[11] R. U. Valente et al., "Status on the development of the Nb_3Sn 12 T Falcon Dipole for the FCC-hh," *IEEE Trans. Appl. Supercond.*, vol. 34, no. 3, May 2024, Art. no. 4900405, doi: 10.1109/TASC.2023.3338166.

[12] S. Farinon et al., "Advancements in Nb_3Sn 12 T cos-theta Dipole development for next-generation accelerators: The INFN-CERN collaboration on the FalconD project," *IEEE Trans. Appl. Supercond.*, vol. 35, no. 5, Aug. 2025, Art. no. 4001905, doi: 10.1109/TASC.2024.3520944.

[13] S. Russenschuck, *ROXIE: Routine for the Optimization of Magnet X-Sections, Inverse Field Calculation and Coil End Design*. Geneva, Switzerland: CERN, 1999, doi: 10.5170/CERN-1999-001.

[14] S. Russenschuck, *Field Computation for Accelerator Magnets: Analytical and Numerical Methods for Electromagnetic Design and Optimization*. Hoboken, NJ, USA: Wiley, Inc., 2011.

[15] O. S. Bruning et al., *LHC Design Report*. Geneva, Switzerland: CERN, 2004, doi: 10.5170/CERN-2004-003-V-1.

[16] A. P. Foussat et al., "High field cos-theta Falcon D-C Dipole magnet development at CERN," presented at the MT 29 2025, Boston, MA, USA, Jul. 1–6, 2025, Paper MT29-Fri-Mo-Or1-02.R1.

[17] D. Pulikowski et al., "Testing mechanical behavior of Nb_3Sn Rutherford cable during coil winding," *IEEE Trans. Appl. Supercond.*, vol. 27, no. 4, Jun. 2017, Art. no. 4802105, doi: 10.1109/TASC.2017.2656179.

[18] D. Pulikowski, F. Lackner, C. Scheuerlein, F. Savary, D. Tommasini, and M. Pajor, "Windability tests of Nb_3Sn Rutherford cables for HL-LHC and FCC," *IEEE Trans. Appl. Supercond.*, vol. 28, no. 3, Apr. 2018, Art. no. 4003905, doi: 10.1109/TASC.2018.2795583.